Experimental and theoretical insight into the soot tendencies of the methylcyclohexene isomers

Seonah Kim[a*], Gina M. Fioroni[a], Ji-Woong Park[b], David J. Robichaud[a], Dhrubajyoti D. Das[c], Peter C. St. John[a], Tianfeng Lu[b], Charles S. McEnally[c], Lisa D. Pfefferle[c], Robert S. Paton[d], Thomas D. Foust[a], Robert L. McCormick[a*]

[a] National Renewable Energy Laboratory, Golden CO 80401 USA

[b] Department of Mechanical Engineering, University of Connecticut, Storrs CT 06269 USA

[c] Yale University, New Haven CT 06520 USA

[d] Chemistry Research Laboratory, University of Oxford, Oxford OX1 3TA UK and Department of Chemistry, Colorado State University, Fort Collins, CO 80523 USA

Corresponding Author: Seonah Kim

15013 Denver W Pkwy, Golden CO 80401

(303) 384-7323

Seonah.kim@nrel.gov

Manuscript submitted to the 37th International Symposium on Combustion

Colloquium: Soot, Nanomaterials, and Large Molecules

Total length of paper: 15 pages

Word Count

Main Text: 3,037 words

References: (25 references + 2) * (2.3 lines/ref) * (7.6 words/line) = 499.0 words

Table 1: (7 lines + 2 lines) * (7.6 words/line) * (1 column) = 60.8 words

Fig. 1: (144.0 mm + 10 mm) * (2.2 words/mm) * (2column) + 42 words = 719.6 words

Fig. 2: (114.3 mm + 10 mm) * (2.2 words/mm) * (2 column) + 101 words = 647.9 words

Fig. 3: (114.3 mm + 10 mm) * (2.2 words/mm) * (2 column) + 31 words = 577.9 words

Fig. 4: (114.3 mm + 10 mm) * (2.2 words/mm) * (2 column) + 31 words = 577.9 words

Total: 6,120.1 words

We will pay color reproduction charges.

Abstract

The formation of soot precursors during combustion of three positional isomers of methylcyclohexene was investigated in flow reactor experiments and through density functional theory simulations. As evidenced by a recently published structure-property model, the sooting tendencies of these compounds differ from those of structurally similar molecules – suggesting new or unusual reaction chemistry. It was demonstrated that 1-methyl-1-cyclohexene and 4-methyl-1-cyclohexene preferentially react via a retro-Diels-Alder pathway leading to ring opening and molecular weight reduction. 3-methyl-1-cyclohexene, which exhibits much higher yield sooting index, preferentially reacts via dehydrogenation to cyclohexadienes and toluene – consistent with higher soot formation. It was demonstrated that the relative stability of the first radical intermediate plays a considerable role in determining the branching ratio between formation of soot precursors and ring opened retro-Diels-Alder reaction products. This study underscores the importance that small structural features can have in determining the ultimate fate of carbon during combustion processes.

Keywords:

Soot; particulate matter; methylcyclohexene; flow reactor; DFT

1. Introduction

Fine particles emitted from combustion sources have well known negative effects on human health[1] and global warming.[2] Particulate matter (PM) from combustion driven transportation sources such as diesel and spark-ignition (SI) engines are significant contributors to these effects. In modern diesel engines, PM emissions are controlled using particle filters.[3] For SI engines, the drive to improve efficiency requires the use of direct injection (DI) of the fuel to increase engine power density and exploit evaporative cooling to increase knock resistance.[4] However, under some operating conditions, DI can cause PM emissions that are greater than earlier generation port fuel injection systems and modern diesel engines equipped with filters.[5,6] This occurs because fuel spray impingement on the piston or cylinder walls results in locally fuel-rich regions or pool fires that produce large quantities of PM.[7] A particle filter solution is available for DISI engines, but these have not yet seen wide adoption.[8] Changing fuel composition is an alternative solution that could have a large impact on DISI engine PM emissions hence mitigating the need for a costly particle filter solution.[9]

A number of different approaches have been used to predict the PM emission effects of different fuels. These include vehicle emissions indices such as the particulate matter index (PMI), which combine the chemical tendency of each compound to form fine particles (or sooting tendency) with some measure of compound's ability to mix with air.[10] While PMI uses a simple metric for chemical sooting tendency (double bond equivalent), other fuel sooting tendency metrics such as smoke point, threshold sooting index, and oxygen extended sooting index use experimental measurements to determine a molecule's chemical tendency to form soot.[11,12] McEnally and Pfefferle introduced the yield sooting index (YSI) as a more precise, apparatus independent, and easily measured soot formation metric.[13,14] Because there are a large number of molecules for which it is desirable to know YSI, St. John and colleagues developed a quantitative structure−activity relationship (QSAR) model for predicting YSI from molecular

structure.[15,16] In cases where the predictive model fails, it highlights where a compound's sooting tendency differs from structurally similar molecules and can point to new or unusual reaction chemistry that is not captured in the model training set.

The positional isomers of methylcyclohexene (MCHe) – 1-methyl-1-cyclohexene (**1MCHe**), 3-methyl-1-cyclohexene (**3MCHe**), and 4-methyl-1-cyclohexene (**4MCHe**), shown in Fig. 1, are one example of compounds that are not well predicted by the QSAR model. As shown in Table 1, the YSI of **3MCHe** is predicted to within 7 YSI units, while the other two isomers have a much lower measured YSI than predicted by the model. Predictions from the QSAR model are reasonable when compared to the YSIs of similar molecules. For cyclohexene, similar carbon types are found in cyclopentane (YSI=70.2) and cycloheptene (YSI=79.0). The higher prediction for **1MCHe** is due primarily to the tertiary ring carbon, found in other high-sooting molecules like 1-methylcyclopentene (YSI=96.5) or 1-methyl-1,4-cyclohexadiene (YSI=175.6). A unique feature of the reaction chemistry of cyclohexenes is their potential to undergo retro-Diels-Alder (retro-DA) reactions. We have previously shown that the over-prediction of YSI for cyclohexene is likely because its reaction via this pathway to form non-radical linear species is not well captured in the QSAR model.[15] However, the activation energy barriers to retro-DA reactions are very similar for the three MCHe isomers, suggesting that this is not a factor in their different soot formation tendency.[16] A preliminary analysis suggested that the higher sooting tendency of **3MCHe** is caused by a lower energy barrier for initial hydrogen extraction and/or for breaking of the C–C bond of the methyl group. Both reactions lead to faster formation of polyaromatic hydrocarbon precursors.

Table 1. Measured and predicted YSI (unified scale) values of the three isomers of methyl cyclohexene and cyclohexene.[16]

Compound		YSI (measured)	YSI (predicted)
Cyclohexene		45.6 ± 2.0	71.1 ± 5.7
1-methyl-1-cyclohexene	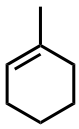	62.0 ± 3.0	108.4 ± 10.4
3-methyl-1-cyclohexene	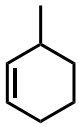	85.0 ± 4.0	77.9 ± 5.8
4-methyl-1-cyclohexene	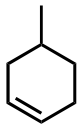	61.0 ± 3.0	80.4 ± 5.8

The purpose of this work is to discover the underlying chemical mechanisms that dictate the different soot formation rates of the three MCHe isomers. This study utilizes flow reactor experiments and density function theory (DFT) calculations to investigate the formation of soot precursors. New pathways are discussed and compared with existing kinetic models.

2. Methods

2.1 Flow Reactor

1MCHe was purchased from Sigma-Aldrich and **3MCHe** and **4MCHe** were purchased from TCI America. All compounds were used neat. Standard solutions of isoprene, 1,4-pentadiene, and trans-1,3-pentadiene were purchased from Sigma-Aldrich and used to verify elution order and positive identification.

The flow reactor is an 13 mm diameter by 75 cm long quartz tube. Organic reactants are fed via a syringe pump with a 22 gauge needle at a flow rate of 10 μL/min. Helium, oxygen, and argon (as a tracer) were metered using mass flow controllers and introduced at the inlet of the reactor along with the fuel. The flow rate of the helium was varied with temperature to maintain a constant residence time. Oxygen was used at a stoichiometric air-to-fuel ratio. The temperature ranged from 850K up to 1100K, in 25K increments. The residence time was 0.35 s. Helium dilution was used to keep the reactor under safe operating conditions (well below the lower explosive limit).

Reaction products were analyzed using two gas chromatographic (GC) systems. The first was a 6890 series II GC (Agilent Technologies) equipped with two 60m x 0.25 μm x 0.25 μm DB-1 wax columns for dual mass spectrum (MS) and flame ionization detector (FID) detection. The GC/MSFID system directly samples effluent from the reactor through a heated 4' transfer line equipped with a 6-port sampling valve. This GC system is capable of analyzing the >C4 hydrocarbon products as well as some oxygenated species. Standards of the MCHe and benzene were run through the reactor system for calibration. 1,4-pentadiene, trans-1,3-pentadiene, and isoprene were also run for elution order purposes. A sample of dicyclopentadiene (Sigma Aldrich) was dissolved in dichloromethane and injected at 400°C resulting in the formation of the cyclopentadiene monomer which was also used for retention time verification.

A second GC system was utilized to quantify the <C4 hydrocarbons and CO_2 and CO. The effluent gas was collected in a 3.2 L summa canister which was injected on a secondary GC system. This GC is equipped with a FID for analysis of C1-C5 hydrocarbons, and two thermal conductivity detectors (TCD) for analysis of permanent gases and water. Separation was by proprietary columns from Wasson-ECE Instrumentation, Fort Collins, CO. Note that this system is not able to identify or quantify acetylene and therefore we are not addressing any potential role that acetylene might have in soot formation from the

methyl cyclohexene isomers. The GC responses for reactants and products were calibrated using purchased gas standards of known concentration.

2.2 Computational methods

We performed DFT calculations using Gaussian 09[17] for each of the MCHe isomers including relative energies for some important radical species and retro-DA reaction pathways. Geometry optimizations along the reaction pathways were conducted with the hybrid GGA B3LYP density functions and the 6-311++G(d,p) basis sets. The composite G4[18] methods for DFT calculations of all 3 isomers including reactants, products, and transition states were followed to fully optimize all stationary points. Composite G4 was chosen to give radical formation enthalpies closest to values recommended in the Active Thermochemical Tables compared to other methods, and gives the smallest confidence intervals against experimental formation enthalpies of 38 open- and 45 closed-shell species (4.5 and 6.2 kJ mol^{-1}, respectively, as shown in Simmie *et al.*).[19] The transition states were confirmed by one imaginary frequency and the intrinsic reaction coordinate (IRC) calculations were performed to relate the relevant reactant and product complexes.

3. Results and Discussions

Results of flow reactor experiments are shown in Fig. 1. Fig. 1a shows reactant concentration as a function of temperature. **3MCHe** is slightly more reactive in this experiment (although all three isomers have essentially identical cetane numbers of 25 to 26). Fig. 1b shows concentrations of the expected retro-DA reaction products. Ring opening and molecular weight reduction occurring in retro-DA is moving away from particle formation precursors – as compared to dehydrogenation reactions that preserve the ring to form cyclic dienes and aromatics. **1MCHe** and **4MCHe** react to a much greater extent

via retro-DA than **3MCHe**, in agreement with the earlier proposal that **3MCHe** will preferentially undergo hydrogen extraction or breaking of the methyl group C-C bond to explain the higher YSI of **3MCHe**.[16] Additionally, as shown in Fig. 1c **3MCHe** produces a much greater yield of cyclic dienes, primarily cyclopentadiene and methyl cyclopentadienes. Cyclopentadienes are likely derived from cyclopentadienyl radicals that can couple directly to form naphthalene.[20] Cyclohexadiene was identified but at extremely low levels (only 0.1% of chromatogram area in the maximum case). Fig. 1d shows total aromatics (benzene, toluene, ethyl benzene, styrene, and xylenes) which are highest at all temperatures for **3MCHe**.

To identify which reaction pathways of MCHe isomers are currently included in the 2014 Lawrence Livermore National Laboratory (LLNL) MCHe chemical kinetic model,[21] a reaction pathway analysis was performed by simulating perfectly stirred reactors (PSR) using the CHEMKIN package.[22] The PSR was simulated at equivalence ratio of 2, ambient pressure and inlet temperature (T) of 300 K, and reaction pathway was analyzed at T≈1756 K and residence time of 0.1 s. It was aimed at differentiating soot precursor pathways, specifically toluene vs. retro-DA reaction pathways – not at simulating the experimental reactor. In general, oxidation was by O_2, O, and OH. The hydroxyl radical is shown as the primary oxidant under the fuel rich conditions,[23,24,25] but the radicals formed (i.e. abstraction by OH, R, H, HO_2, O, O_2, etc.) are inconsequential to the conclusion of this study and the pathways we were investigating. Therefore, in all our energy calculations, we made the simplifying assumption that the hydroxyl radical was the exclusive chain propagator.

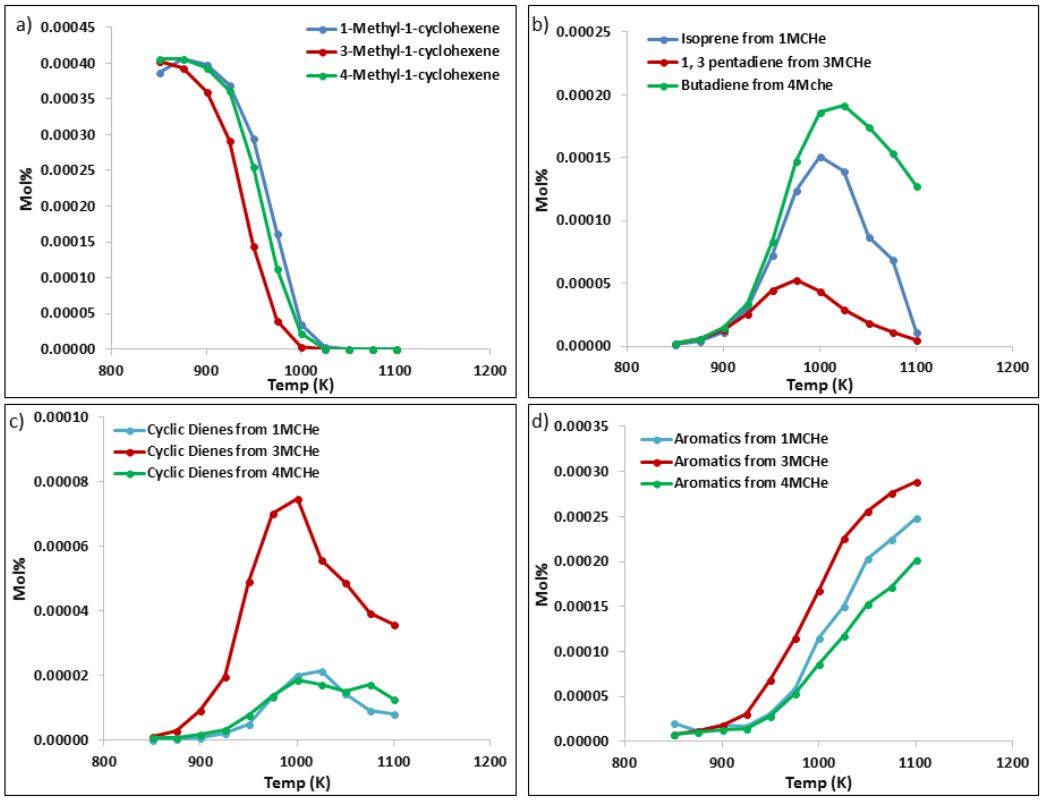

Fig. 1. Reactant and product concentrations as a function of temperature: a) MCHe reactants, b) expected retro-DA products (higher molecular weight), c) total cyclic dienes (cyclopentadiene, methyl cyclopentadiene isomers, and cyclohexadienes), and d) total aromatics (benzene, toluene, ethyl benzene, styrene, and xylenes).

The competing reaction pathways of **3MCHe** to form toluene and retro-DA products (ethylene and 1,3-pentadiene) are shown in Fig. 2. The barriers for H-abstraction from **3MCHe** by OH radicals are small (<5kcal/mol) and result in the formation of 5 different radical species (**3MCHe_1rad**, **3MCHe_4rad**, **3MCHe_2rad**, **3MCHe_3rad**, **3MCHe_0rad**) with Gibbs free energy of reactions of -39.0, -36.8, -22.3, -22.9 and -19.6 kcal/mol, respectively. Two of the radical species (**3MCHe_1rad** and **3MCHe_4rad**) are approximately 20 kcal/mol more stable than the rest of radical species due to the resonance stabilization between the radical site and the ring double bond. Unimolecular [1,2]H-shift rearrangements barriers

are also shown in Fig. 2 depicted by red lines connecting two of the radical species. The activation energy barriers for [1,2]H-shift rearrangements from the more stable radicals (**3MCHe_1rad** and **3MCHe_4rad**) to the less stable radical species (**3MCHe_2rad**, **3MCHe_3rad**, **3MCHe_0rad** are high (48.0, 51.4, and 46.7 kcal/mol, respectively) compared to the activation energy barriers of the reverse reaction (31.3, 32.0, and 32.8 kcal/mol, respectively). Therefore, in the absence of any rapid secondary reaction pathways, the thermodynamic driving force should result in a higher population density of the two stable radical species (**3MCHe_1rad** and **3MCHe_4rad**) which are not proposed in 2014 MCHe LLNL mechanism.[21] As shown in Figure 2, [1,2]H-shifts are typically assumed to be uncompetitive under autoignition conditions: however, at the temperatures considered in our simulations the [1,2]H-shift transition states are similar in stability to C-C β-scission. More pathways are accessible and in competition at higher temperatures.

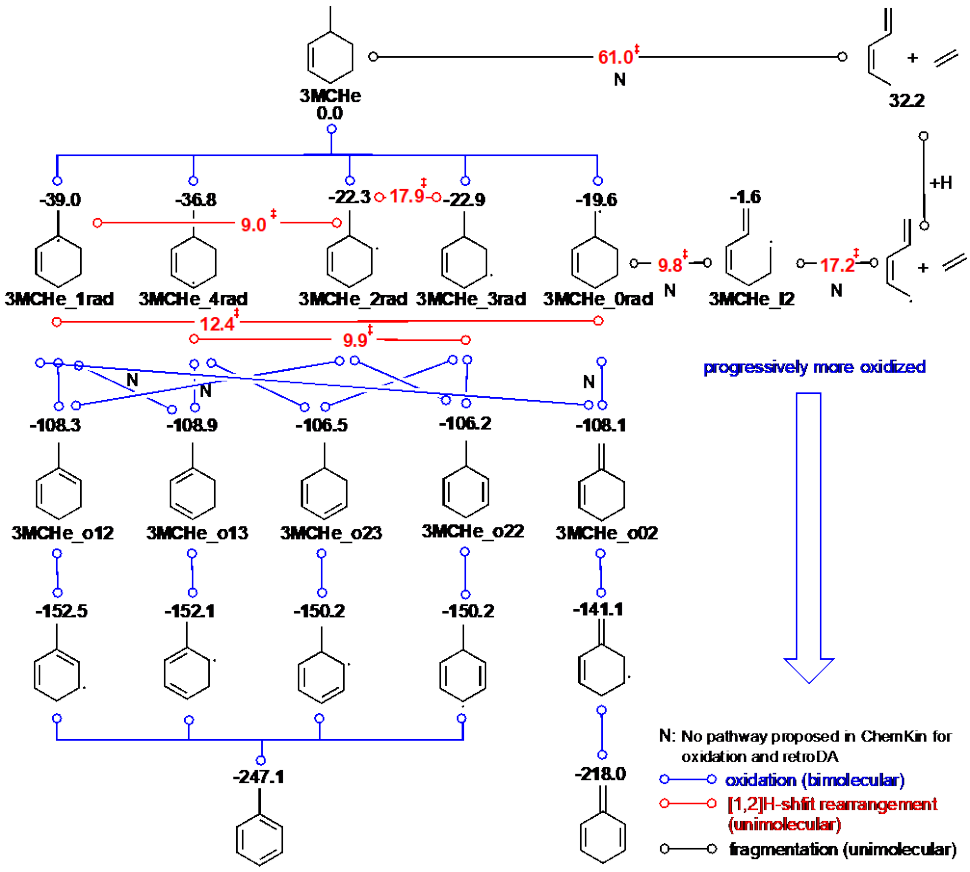

Fig. 2. Reaction pathways of **3MCHe** to form possible soot precursors with retro-DA reaction products as a competing pathway (T≈1756 K). All lines indicate elementary steps. Blue lines indicate a bimolecular oxidation reaction with an OH radical. Unimolecular [1,2]H-shift rearrangements are shown in red lines. Black lines indicate a unimolecular retro-DA reaction either concerted or step-wise mechanism. All energies were calculated using the composite G4 theory and are reported in kcal/mol relative to **3MCHe**. Black energies are local minima while red energies are activation free energy barriers. "N" denotes pathways that are missing from the 2014 LLNL MCHe chemical kinetic model.[21]

For the retro-DA reaction, two possible pathways, concerted and step-wise, are proposed in Fig. 2. The concerted mechanism directly occurs from reactant (**3MCHe** in Fig. 2) to produce ethylene and 1,3-pentadiene with a 61.0 kcal/mol activation energy barrier. In step-wise retro-DA, the reaction initiates with a ring opening of **3MCHe_0rad** followed by C-C bond breaking to produce 1,3-pentadiene radical and ethylene with a 29.4 kcal/mol barrier height (relative to **3MCHe_0rad**). 1,3-pentadiene radical reduces with hydrogen to produce 1,3-pentadiene, and the overall computed ΔG value is 32.2 kcal/mol. Alternatively, 1,3-pentaidene radical can eliminate an H atom to cyclize and form cyclopentadiene (not shown). The step-wise retro-DA could be a competing pathway for formation of the soot precursor toluene. However as previously discussed, **3MCHe_0rad** prefers to isomerized to **3MCHe_1rad** via a [1,2]H-shift rearrangement due to the resonance stabilized radical species than the retro-DA pathway. Further oxidation of the five radicals (**3MCHe_1rad**, **3MCHe_4rad**, **3MCHe_2rad**, **3MCHe_3rad**, **3MCHe_0rad**) can result from either OH abstraction or unimolecular C-H scission. Regardless, the end result is the same: a methylcyclohexadiene species that can rapidly oxidize further to soot precursor toluene or 3-methylene-1,4-cyclohexadiene.

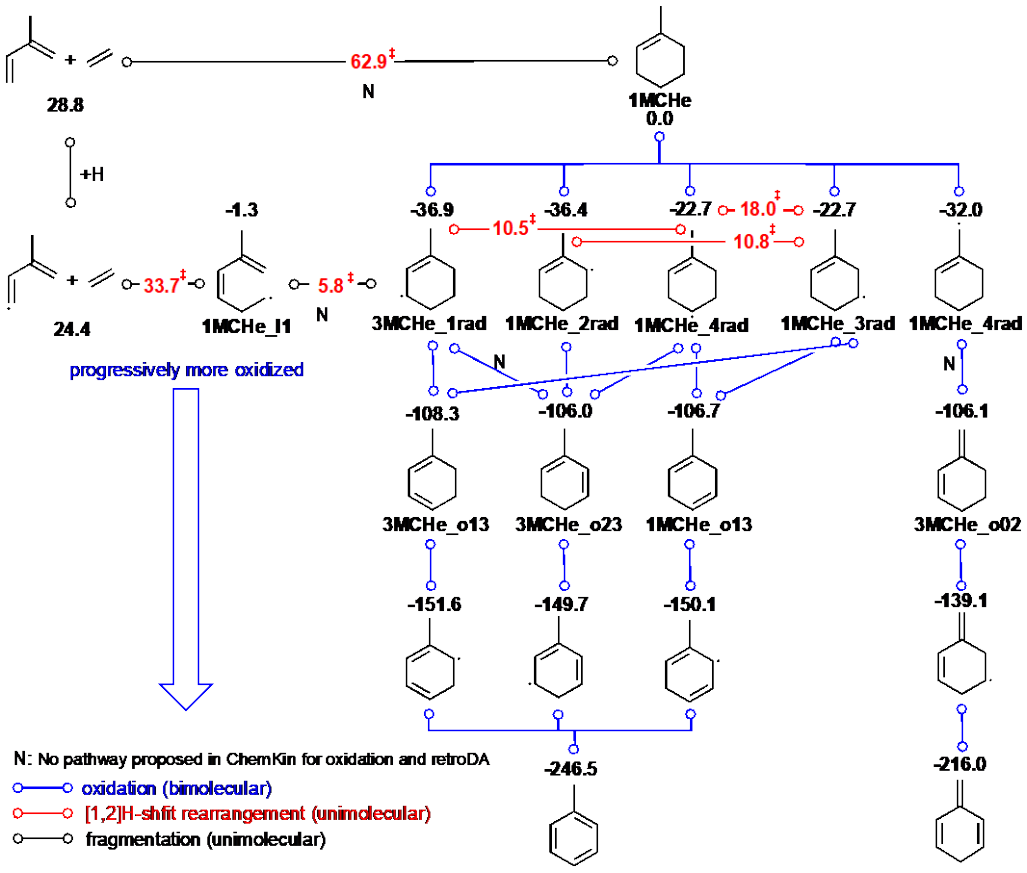

Fig. 3. Reaction pathways of **1MCHe** (T≈1756 K). Notation is consistent with Fig. 2. All energies were calculated using the composite G4 theory and are reported in kcal/mol relative to **1MCHe**.

Detailed reaction pathways for **1MCHe** and **4MCHe** are shown in Figs 3 and 4 respectively. Recall that these two species exhibit similar experimental YSI values (see Table 1). Both **1MCHe** and **4MCHe** form different radical species and intermediates because of its different double bond position. The barrier of reaction and heats of reactions are similar between the three isomers, including the retro-DA pathway (61-63 kcal/mol). The primary difference is in the stability of the radical intermediate that can undergo the stepwise retro-DA pathway. In **3MCHe**, it is the less-stable **3MCHe_0rad** that can undergo the retro-DA reaction. The thermodynamic driving force shifts the population density away from that radical and toward the more stable **3MCHe_1rad**, which can only proceed via oxidation toward toluene formation. In the case of **1MCHe** and **4MCHe**, the more stable radical is the exact species that can undergo the

stepwise retro-DA pathway or toluene formation. Therefore, these two isomers are able to divert significant product away from toluene (soot precursor) and toward retro-DA products routes (isoprene and ethylene for **1MCHe** and butadiene and propylene for **4MCHe**). In comparison with experimental results (Fig. 1) we see that this is exactly the case, **3MCHe** leads to a significantly higher amount of cyclic dienes and aromatics (precursors to toluene) in Fig. 1c and 1d and a concomitant lower production of retro-DA products (1,3-pentadiene in Fig. 1b) than the other two isomers.

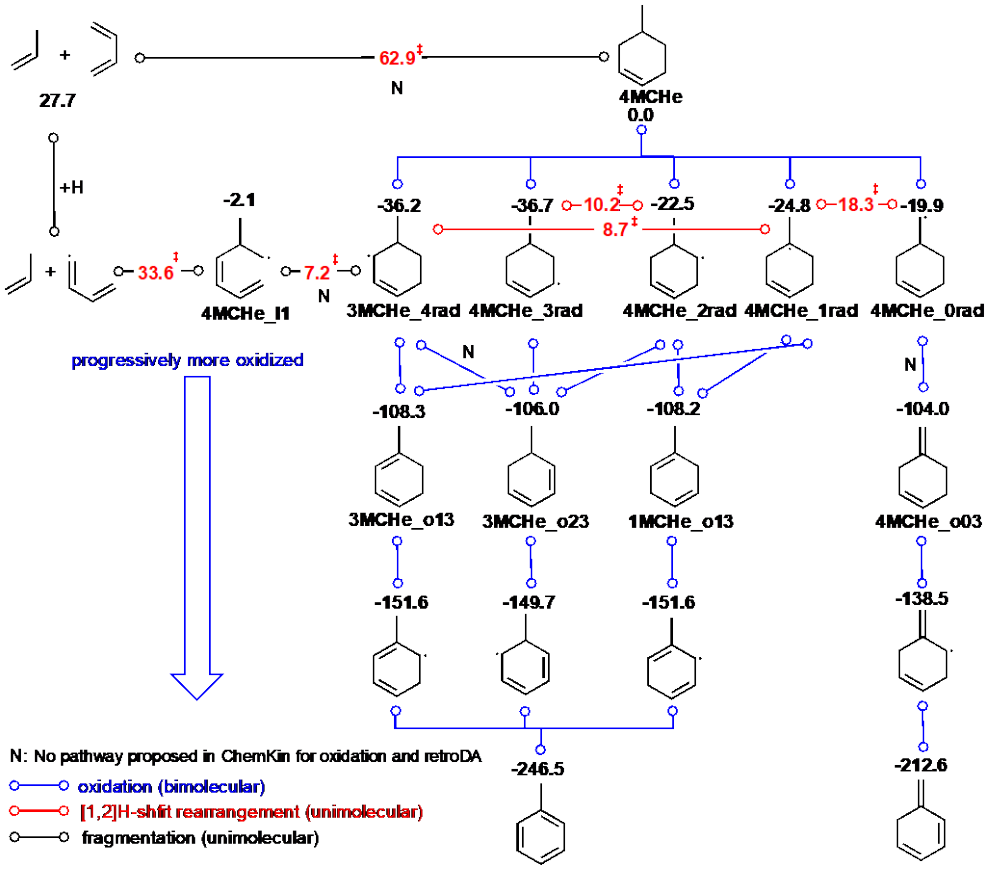

Fig. 4. Reaction pathways of **4MCHe** (T≈1756 K). Notation is consistent with Fig. 2. All energies were calculated using the composite G4 theory and are reported in kcal/mol relative to **4MCHe**.

4. Conclusions

A comparison of experimental YSI values for the three methyl cyclohexene isomers with predictions from structure-property model shows that the model over predicts YSI significantly for **1MCHe** and **4MCHe**

but provides a reasonable estimate for **3MCHe**. Flow reactor experiments show that **1MCHe** and **4MCHe** form retro-DA products to a much greater extent than **3MCHe**. **3MCHe** forms higher levels of cyclic diene and aromatic soot precursors. The theoretical analysis demonstrates that the relative stability of the first radical intermediate plays a considerable role in determining the branching ratio between soot precursors (e. g. toluene) and retro-DA products (low sooting) formation pathways.

5. Acknowledgements

This work was authored in part by Alliance for Sustainable Energy, LLC, the manager and operator of the National Renewable Energy Laboratory for the U.S. Department of Energy (DOE) under Contract No. DE-AC36-08GO28308. Funding provided by U.S. Department of Energy Office of Energy Efficiency and Renewable Energy Bioenergy Technologies Office. The views expressed in the article do not necessarily represent the views of the DOE or the U.S. Government. The U.S. Government retains and the publisher, by accepting the article for publication, acknowledges that the U.S. Government retains a nonexclusive, paid-up, irrevocable, worldwide license to publish or reproduce the published form of this work, or allow others to do so, for U.S. Government purposes. This research was conducted as part of the Co-Optimization of Fuels & Engines (Co-Optima) project sponsored by the U.S. Department of Energy (DOE) Office of Energy Efficiency and Renewable Energy (EERE), Bioenergy Technologies and Vehicle Technologies Offices. C.S.M. and L.D.P are also supported by the National Science Foundation (NSF) under Grant No. CBET 1604983. Computer time was provided by the NSF Extreme Science and Engineering Discovery Environment (XSEDE), Grant No. ACI-1053575 and by the National Renewable Energy Laboratory Computational Science Center.

6. References

[1] C.A. Pope, M. Ezzati, D. W. Dockery, N. Engl. J. Med. 360 (4) (2009) 376–386.

[2] V. Ramanathan, G. Carmichael, Nature Geoscience 1 (2008) 221–227.

[3] I. A. Khalek, M.G. Blanks, P.M. Merritt, B. Zielinska, J. Air Waste Manag. Assoc. 65(8) (2015) 987 – 1001.

[4] T.G. Leone, J.E. Anderson, R. S. Davis, A. Iqbal, Environ. Sci. Technol. 49 (2015) 10778−10789.

[5] P. Price, R. Stone, T. Collier, M. Davies, SAE Technical Paper 2006-01-1263 (2006).

[6] B. Liang, Y. Ge, J. Tan, X. Han, L. Gao, L. Hao, W. Ye, P. Dai, J. Aerosol Sci. 57 (2013) 22–31.

[7] E. Stevens, R. Steeper, SAE Technical Paper 2001-01-1203 (2001).

[8] T.W. Chan, E. Meloche, J. Kubsh, R. Brezny, Environ. Sci. Technol. 48 (10) (2014) 6027–6034.

[9] M. Ratcliff, J. Burton, P. Sindler, E. Christensen, L. Fouts, G. M. Chupka, R. L. McCormick, SAE Int. J. Fuels Lubr. 9(1) (2016) 59–70.

[10] K. Aikawa, T. Sakurai, J. and Jetter, SAE Int. J. Fuels Lubr. 3(2) (2010) 610–622.

[11] Y. Yang, A.L. Boehman, R.J. Santoro, Combust. Flame 149 (2007) 191–205.

[12] E.J. Barrientos, J.E. Anderson, M. M. Maricq, A. L. Boehman, Combust. Flame 167 (2016) 308–319.

[13] C.S. McEnally, L.D. Pfefferle, Combust. Flame 148 (2007) 210–222.

[14] C.S. McEnally, L.D. Pfefferle, Environ. Sci. Technol. 45 (2011) 2498–2503.

[15] P.C. St. John, P. Kairys, D.D. Das, C.S. McEnally, L.D. Pfefferle, D.J. Robichaud, M.R. Nimlos, B.T. Zigler, R.L. McCormick, T.D. Foust, Y.J. Bomble, S. Kim, Energy & Fuels 31 (9) (2017) 9983–9990.

[16] D.D. Das, P. C. St. John, C.S. McEnally, S. Kim, L.D. Pfefferle, Combust. Flame, submitted, available on the engrXiv preprint server at https://dx.doi.org/10.17605/OSF.IO/9WQFN.

[17] M.J. Frisch, G.W. Trucks, H.B. Schlegel, G.E. Scuseria, M.A. Robb, et al. 2009. Gaussian 09, Revision D.01; Gaussian, Inc. In Gaussian 09, Revision B.1; Gaussian, Inc. Wallingford, CT.

[18] L.A. Curtiss, P.C. Redfern, K. Raghavachari, J. Chem. Phys. 126 (2007) 084108.

[19] J. M. Simmie, K. P. Somers, J. Phys. Chem. A 119 (28) (2015) 7235-7246.

[20] A.M. Scheer, C. Mukarakate, D.J. Robichaud, G.B. Ellison, M.R. Nimlos, J. Phys. Chem. A 114(34) (2010) 9043–9056.

[21] B.W. Weber, W.J. Pitz, M. Mehl, E.J. Silke, A.C. Davis, C.-J. Sung 2014. Combust. Flame 161 (2014) 1972–83.

[22] CHEMKIN-PRO 17.2, ANSYS, Inc.: San Diego, 2016.

[23] A.D. Sediako, C. Soong, J.Y. Howe, M.R. Kholghy, M.J. Thomson, Proc. Combust. Inst. 36 (2017) 841–51.

[24] K.G. Neoh, J.B. Howard, A.F. Sarofim, In Particulate Carbon: Formation During Combustion, ed. DC Siegla, GW Smith, Springer US, Boston, 1981, p. 261–82.

[25] J.S. Lighty, V. Romano, A.F. Sarofim, Combustion Generated Fine Carbonaceous Particles (Proceedings of An International Workshop Held in Villa Orlandi, Anacapri, May 13-16, 2007), 2009, p. 523–36.